LIMNOLOGY and OCEANOGRAPHY

Increasing nutrient stress reduces the efficiency of energy transfer through planktonic size spectra

Angus Atkinson [ORCID],[1]* Martin K.S. Lilley,[2] Andrew G. Hirst,[3,4] Andrea J. McEvoy,[1] Glen A. Tarran,[1] Claire Widdicombe,[1] Elaine S. Fileman,[1] E. Malcolm S. Woodward,[1] Katrin Schmidt,[5] Tim J. Smyth,[1] Paul J. Somerfield[1]

[1]Plymouth Marine Laboratory, Plymouth, Devon, UK
[2]Sustainable Aquaculture Futures, Cefas and University of Exeter Collaborative Centre, College of Life and Environmental Sciences, University of Exeter, Exeter, Devon, UK
[3]School of Environmental Sciences, University of Liverpool, Liverpool, UK
[4]Centre for Ocean Life, National Institute for Aquatic Resources, Technical University of Denmark, Lyngby, Denmark
[5]University of Plymouth, Plymouth, Devon, UK

Abstract

Size-spectral approaches quantify the efficiency of energy transfer through food webs, but theory and field studies disagree over how changes in temperature, nutrients, and extreme weather impact on this efficiency. We address this at two scales: via 6 years of weekly sampling of the plankton size spectrum at the Plymouth L4 shelf sea site, and via a new, global-scale, meta-analysis of aquatic size spectra. The time series showed that with summertime nutrient starvation, the energy transfer efficiency from picoplankton to macroplankton decreased (i.e., steepening slopes of the size spectra). This reflected increasing dominance by small cells and their microbial consumers. The extreme storms in winter 2013/2014 caused high metazoan mortality, steep size-spectral slopes, and reduced plankton biomass. However, recovery was within months, demonstrating an inbuilt resilience of the system. Both L4 and our meta-analysis showed steep slopes of normalized size spectra (median −1.11). This reflects much lower values, either of trophic transfer efficiency (3.5%) or predator–prey mass ratio (569), compared to commonly quoted values. Results from the meta-analysis further showed that to represent energy transfer faithfully, size spectra are best constructed in units of carbon mass and not biovolume, and span a mass range of $> 10^7$. When this range is covered, both the meta-analysis and time series show a dome-shaped relationship between spectral slopes and plankton biomass, with steepening slopes under increasingly oligotrophic and eutrophic conditions. This suggests that ocean warming could decrease the efficiency of energy transfer through pelagic food webs via indirect effects of increasing stratification and nutrient starvation.

Climate change and the efficiency of energy transfer through the plankton

In a warming climate, increases in ocean temperature, stratification, nutrient shortage, and the frequency of extreme climatic events are predicted (Coumou and Rahmstorf 2012; Holt et al. 2016; IPCC 2019). Several studies have measured how such factors affect the food web, for example, through reductions in body size associated with warming (Daufresne et al. 2009; Li et al. 2009). However, a challenge facing ecologists is that changing temperatures can have multiple direct and indirect effects on the food web. For example, temperature can affect zooplankton both directly through their physiology, and indirectly, for example, through changing stratification and thus nutrient supply, which impact on the abundance, size, and quality of their food (Schmidt et al. 2020).

Both direct and indirect effects of climatic warming impact on the efficiency of energy transfer through food webs (Morán et al. 2010), making this a key emergent property to assess. The rate of energy loss as it passes through a food web reflects a series of inefficiencies in organism metabolism, trophic

Additional Supporting Information may be found in the online version of this article.

transfer, and the number of these transfers within any given size spectrum. To address such processes, size-spectrum approaches have had a long history of development (Elton 1927; Sheldon et al. 1972; Platt and Denman 1978; Sprules and Barth 2016; see following section "Theoretical overview"). One of their key advantages is that the slope of the size spectrum (i.e., the rate of decrease in biomass with increasing organism size) provides a measurable index of the combined effects of the various inefficiencies, each of which is very hard to measure across a whole assemblage (Jennings et al. 2002).

Given the importance of body size as a central and simplifying framework, a large amount of theoretical and modeling work, as well as empirical studies, have been devoted to understanding the controls on size spectra (e.g., Zhou and Huntley 1997; Andersen 2019). These have come to rather conflicting conclusions on the behavior of size spectra, and there is currently no consensus on the key factors driving the slope of the spectra. For example, the interrelationships among body size, temperature, and metabolic rate (Brown et al. 2004) have led to projections that size-spectral slopes are more steeply negative (less efficient energy flow) at higher temperatures, but this is not clearly supported by empirical studies (García-Comas et al. 2014). Likewise, stable (mainly oligotrophic) systems have been suggested to have steeper slopes (Jennings and Mackinson 2003), and while this seems to be supported in freshwater systems (Sprules and Munawar 1986), it is not clearly supported in the ocean (San Martin et al. 2006*a*, *b*; Kenitz et al. 2018). Because most of the empirical studies provide only a snapshot of a system, often not in a steady state, there is a need to provide wider scale insights, both from time series of size spectra spanning all plankton (Sprules and Barth 2016), and from wider-scale literature syntheses that average out the underlying variability (San Martin et al. 2006*b*).

Measuring size spectra across a sufficient range of body size and at large spatial–temporal scales is nontrivial (Sprules and Barth 2016). While many studies have measured size spectra, few span both a large range of body size and large time or space scales. The very wide range of slopes of planktonic size spectra that have been reported, plus the lack of consensus between studies, reflects methodological issues as well as environmental variability (Quinones et al. 2003). For instance, slopes are being increasingly derived from single instruments that can sample only a portion of the full planktonic size spectrum, and in units of biovolume rather than carbon, and these measurement units can yield different slopes to those based on carbon units (Quinones et al. 2003). To determine whether there is any systematic variation in energy transfer efficiency through plankton using size-based approaches, we first need to separate methodological issues from environmental controls.

Given that body size is such a fundamental trait (Jennings et al. 2002; Brown et al. 2004; Brose et al. 2019), we hypothesize that size-spectral approaches can indeed be used to quantify how the efficiency of energy transfer responds to climatic variability. We further hypothesize that stress from summer nutrient shortage and extreme weather will depress the efficiency of energy flow through the planktonic size spectrum. We approached these hypotheses at two scales. First, we studied the behavior of a full planktonic size spectrum (from bacteria to macrozooplankton) at a seasonally stratifying shelf site at weekly resolution for 6 years. While seasonal change at a single site is not an analogue of climate change, it does offer a "natural experiment" on the effects of increasing temperature and nutrient shortage, as well as superimposed extreme storm events. Frequent measurements of the ensuing changes in size structure tell us how climatic variability affects the overall efficiency of energy transfer across the whole size spectrum. Second, at the larger scale, we conducted a meta-analysis of the global plankton literature to place our results into wider context. This allowed us to test some of the key factors that lead to the wide scatter in size-spectral slopes reported, an overview of how efficiently energy is transported through the whole plankton size spectrum, and the key factors that dictate variability in this efficiency.

Theoretical background: The use of body size spectra

Body size is a "master trait," dictating the pace of a suite of biological and biogeochemical processes ranging from nutrient acquisition to particle export (Peters 1983; Blanchard et al. 2017). The importance of body size has been recognized for nearly a century (e.g., Elton 1927; Sheldon et al. 1972; Platt and Denman 1978), but the last few decades have seen an upsurge in size-based approaches to understand impacts ranging from eutrophication to fishing (Trebilco et al. 2013; Sprules and Barth 2016; Blanchard et al. 2017). While a range of size-based models have been developed, with parameterizations of varying complexity (Zhou and Huntley 1997; Banas 2011; Rossberg 2012; Ward et al. 2012), they stem from rather similar basic concepts (Mehner et al. 2018). Thus, the inefficiency of energy transfer at each trophic step, the number of these steps and inefficiency of metabolism act in unison to drive a decline in biomass up through the food web (Kiørboe 2008).

The upsurge in appeal of size-based approaches reflects a series of factors. First, improvements in technology to enumerate particles have helped size-based processing (Dai et al. 2016). Second, size-based models allow a degree of simplification of multiple, often poorly known, processes for a plethora of component individuals in an aquatic assemblage (Ward et al. 2012). Third, size structure is easier to measure than other properties of a whole assemblage, namely trophic transfer efficiency, predator–prey mass ratios, or the mass exponent of production (growth) scaling, yet it provides insights into their combined effects on food web efficiency (Jennings et al. 2002).

Based on the conceptual and mathematical advances made by Reuman et al. (2008), the interconnections between allometric scaling of production (growth rate), trophic transfer efficiency, predator–prey mass ratio, and the slope of biomass spectra are underpinned both theoretically and empirically (Trebilco et al. 2013; Mehner et al. 2018). From the scaling of production (growth rate) with body mass (b; Brown et al. 2004), the predator: rey mass ratio (PPMR), and the trophic transfer efficiency (TTE; Mehner et al. 2018), a measurable property of the assemblage emerges, namely the rate of reduction of total biomass with increasing organism size. If this rate of reduction is expressed as the slope, S, of the normalized biomass size spectrum (NBSS) then (Eq. 1 is from Mehner et al. 2018):

$$S = \left[\mathrm{Log}_{10}\,(\mathrm{TTE}) / \mathrm{Log}_{10}\,(\mathrm{PPMR}) \right] - b. \tag{1}$$

Thus, low values for TTE and high values of b both lever toward overall inefficiency of energy passage through the food web, and together with low values for PPMR, all act to steepen the rate of reduction in biomass with increasing body size. In aquatic food webs each of these variables has been measured or estimated based on compilations of large amounts of data or, as in the case of b, also derived from metabolic theory (Brown et al. 2004). Commonly quoted values are $b = 0.75$, TTE $= 0.1$, and PPMR $= 10^4$ (Mehner et al. 2018). Substituting these values into Eq. 1 yields a slope of the NBSS of -1. This "benchmark" value is indeed in line with a long history of empirical measurements. A convergence on NBSS values at around -1 has been noted for decades, originating from Sheldon et al.'s (1972) observation that there were roughly equal biomasses in logarithmically equal intervals of body mass.

Methods

Overview of the L4 monitoring site

The coastal site L4 is in the northwest English Channel, 13 km SSW of Plymouth with water ~ 54 m deep. Weekly sampling has been ongoing at L4 since 1988 (Harris 2010), initially focused on zooplankton (Eloire et al. 2010), but expanded in recent years to cover more of the size spectrum (Smyth et al. 2015). Six years of data are analyzed here, comprising 275 sampling time points spanning 2009–2014. This period had a continuous, near weekly, collection of samples that were analyzed in a consistent manner. More detailed descriptions of sampling and analysis methods are provided in Supporting Information Section S1, but methods included flow cytometry (picoplankton and nanoplankton), microscope analysis of Lugol's-preserved water samples (nanoplankton and microplankton) and microscope analysis of WP2 net samples (mesoplankton and macroplankton).

Weekly sampling of L4 begins with a CTD cast collecting water samples at standard depths of 2, 10, 25, and 50 m. This is followed by a pair of slow (~ 0.2 m s^{-1}) hauls with a 200-μm mesh, 57 cm diameter, WP2 net from 50 m to the surface. In recent years we have been using a 63-μm net haul towed slowly from 50 m to the surface, to provide improved sampling of micrometazoa that are poorly enumerated, either in the WP2 net catches or Lugol's preserved water samples. These samples were used to test the effect of including this missing fraction from the NBSS (Supporting Information Section S2), but not in the final analyses due to incomplete coverage of time points.

Biomass spectrum: Overall approach

In common with most plankton time series, L4 analysis is based on taxonomic categories rather than purely size-based approaches. While purely size-based data have been recommended for the construction of NBSS (Quinones et al. 2003; Trebilco et al. 2013), we follow the more taxonomically based method of Mehner et al. (2018), Tarling et al. (2012). We therefore enumerated many (393) individual categories based dually on size and taxonomic identity. This approach has several advantages. A key point is that inshore plankton assemblages in dynamic environments, such as at L4, can include variable, and sometimes substantial, proportions of nonliving material including carcasses (Maud et al. 2018); this proportion is best distinguished, and excluded, based on expert microscopic analysis. Second, our more taxonomic-based approach helps to diagnose the "anatomy" of the size spectrum and the taxa contributing to its variability. We argue that the fine granularity of our analysis, with 393 live cell categories enumerated consistently, across 275 time points, allows a perspective on temporal resolution that is rarely possible in purely size-based studies.

A key consideration for any size-spectral analysis is the spatial extent of the assemblage under study. Given the fine temporal resolution of our sampling of an assemblage dominated by pico- and nano-sized cells, we selected the upper, more productive, 10-m layer sampled by bottles both for flow cytometry and microscope analysis of protists. The larger mesozooplankton, however, are more mobile, so we used whole (50 m) depth-integrated net samples. Because the vertical extent of measured assemblages is an important consideration (Quinones et al. 2003; Trebilco et al. 2013), we compared our NBSS with that based on full-depth integration of the water bottle flow cytometry samples (Supporting Information Section S2). The underlying pattern of seasonality was very similar, whether NBSS was based on 10 m depth only or the whole water column, providing reassurance that our results are robust for this issue.

Biomass spectrum: Calculations

For each taxon counted at each time point, we multiplied numerical density (no. m^{-3}) by their individual carbon mass (μg C individual^{-1}) to derive biomass density (μg C m^{-3}; see Supporting Information Section S1). We then averaged the weekly resolution samples into months to derive 72 monthly NBSS (mean 3.82 samples per month, range 1–5). December

2011 had only one mesozooplankton and no microplankton samples, so this month's NBSS was calculated from flow cytometry and mesoplankton data only. June 2013 was characterized by a dense bloom of *Phaeocystis* spp., gelatinous colonies of which clogged the plankton nets decreasing filtration efficiency. We therefore excluded this month due to our inability to sample the whole size-spectrum quantitatively.

To construct the NBSS, total carbon biomass (μg C) was calculated within 0.5 $\log_{10}$ mass bins, by month and year, and then divided by the width of the unlogged mass bin to normalize the data. These values were then plotted in log space and ordinary least squares regressions calculated to determine NBSS slopes for each month (Sprules and Barth 2016). Other approaches, including maximum likelihood estimation, have since been recommended (Edwards et al. 2017), but we decided to use the more commonly applied least squares regression on binned data, to make our results directly comparable to previous work summarized in our meta-analysis. To examine seasonal behavior of the NBSS, we calculated the relationship between the NBSS slope and its elevation, which provides an index of biomass. For the latter we selected the elevation (*y*-value) of the NBSS at the geometric mean midpoint of the regression line (i.e., at an *x*-value of -2.75 μg C ind^{-1}). This elevation provides a center point index of plankton biomass that is not sensitive to the slope itself (Sprules and Barth 2016).

Meta-analysis

While some studies have tabulated a selection of NBSS slopes from the literature (Dai et al. 2016) or from multiple environments (e.g., Sprules and Munawar 1986), we are not aware of any systematic, large-scale compilation and meta-analysis of planktonic size spectra spanning marine and freshwater habitats. Therefore, we surveyed the marine and freshwater literature for published studies of NBSS slopes of planktonic size spectra. The extracted data spans a large range of marine and freshwater habitats from the tropics to the poles and both hemispheres.

Studies were selected where data were presented (or extractable from the figures) on both NBSS slopes and on the mass or biovolume range used for the size spectrum. Supporting Information Table S2 presents the 40 studies accessed, which provided 282 separate slope values. Each of these slope values pertains to the average value (often of multiple time points or stations) of a specific environment, for example, a monthly average NBSS slope for a time series, or for a specific subregion of a spatial study. As well as basic sampling information such as region, time of year of sampling and sampling depth, we have coded each determination of slope and size range of NBSS as either marine or freshwater, and based either on biovolume or mass.

To test the effects of environmental data on the slopes of the NBSS, we extracted temperature, nutrient, and surface Chlorophyll *a* (Chl *a*) data, where possible, from each publication (Supporting Information Table S2). Unfortunately, these data were too rarely provided to allow a meaningful analysis for the whole data set, with the exception of those studies that analyzed a wide range of body mass. This subset was in any case considered to provide the most robust determinations of NBSS slope (see "Results: meta-analysis"), so we focused our environmental meta-analysis on this subset of data. Supporting Information Table S2 provides a more detailed description of how both the NBSS slopes, and the supporting environmental data were extracted from each publication.

Results

The L4 environment

The L4 site is transitionally stratified, with a thermocline forming typically from May to September, allowing a ~ 10°C seasonal range in surface temperatures (Smyth et al. 2010, 2015; Fig. 1a). While receiving more mixing than more open shelf sites in the Celtic Sea (Schmidt et al. 2020), L4 still experiences macronutrient shortage, with nitrate near the limit of detection typically from June to August. The L4 site often experiences diatom blooms in early summer and dinoflagellate blooms in late summer, albeit with considerable interannual variability in both taxonomic contribution and timing of phytoplankton and zooplankton (Eloire et al. 2010; Widdicombe et al. 2010; Atkinson et al. 2015; Tarran and Brunn 2015).

Figure 1 illustrates the extent of variation in the main plankton functional groups during our 6-year study. Some groups are clearly much more variable than others, with picoplankton and nanoplankton, as well as copepods, displaying relatively low amplitudes of seasonal and interannual variation. Conversely, diatoms, dinoflagellates, gelatinous zooplankton can vary over 10-fold between years within any given month.

L4: Trends in slope and elevation of NBSS

Over the 6 study years, the annual-average NBSS slopes and elevations were remarkably constant (Fig. 2a), with slopes ranging from -1.101 (2010) to -1.117 (2011) and overlapping 95% confidence intervals. By contrast, significant seasonal differences were found in both NBSS slope and elevation, with non-overlapping 95% confidence intervals (Fig. 2b). Average NBSS slopes ranged from -1.082 in March to their steepest values of -1.148 in January. Despite seasonal-annual and interannual variation in NBSS slopes, all 72 values were < -1, with an overall median value of -1.113. All but one of the 6 years showed the same general trend, with a general steepening of NBSS slopes during the summer (Fig. 2c) and an increase in elevation from January to about August (Fig. 2d). The 2012 summer was anomalous, being particularly wet with likely nutrient inputs from rain and river run-off contributing to a particularly long-lasting diatom bloom (Atkinson et al. 2015; Tait et al. 2015). This year was reflected in a relatively stable NBSS slope rather than the more usual summer

dip, and reflected replacement of picoplankton and nanoplankton with microplankton during the summer stratified period.
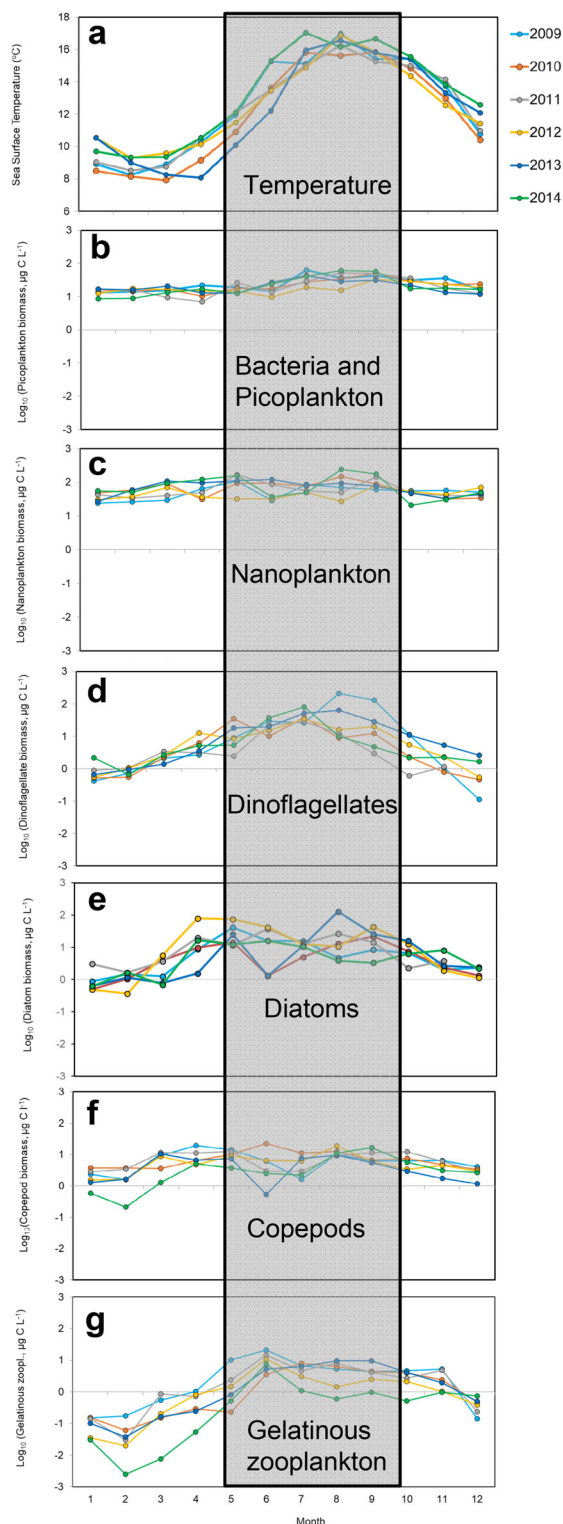
L4: Impacts of the stormy 2013–2014 winter

The 2013–2014 winter had the highest frequency of storms in the United Kingdom for 100 years (Wadey et al. 2014), with a series of storm tracks causing particularly severe damage to the southwest United Kingdom (Kendon and McCarthy 2015). This winter was exceptional, both for the duration of the stormy and wet weather, which lasted from December 2013 to March 2014, and for the severity of the storms themselves. The most energetic period was 8 weeks spanning mid-December 2013 to mid-February 2014, when > 10 m waves caused substantial seabed erosion, wholesale removal of beaches in the Plymouth area and an increase in turbidity (Wadey et al. 2014; Masselink et al. 2016).

Plankton sampling at L4 was able to continue between these storms and the period February 2013–March 2014 was marked by unusually low biomass of metazoans (Fig. 1f,g) but near typical values for the protists (Fig. 1b–e). This was reflected in an initially steep NBSS slope and elevation; abnormally low compared to most of the other winters (Fig. 3a). Importantly, however, the biomass and NBSS slope returned to near-normal levels by April 2014.

L4: Which taxa contribute to variability in the NBSS slope?

Figure 1 presents the component contributions of the main taxa to the biomass spectrum. The key feature throughout the main growth season of increasing water temperatures (March–September) is a progressive steepening of the NBSS slope. Figure 1 shows major increases in bacteria, picoplankton, nanoplankton, and dinoflagellates through this period, but either modest or no increases in metazoan biomass.

To examine which taxa contributed most to the variation in the NBSS slope over time, we used as predictor variables the proportion of total biomass of each of the functional groups. NBSS slope values correlated most strongly with dinoflagellate biomass, accounting for 44% of the slope variation. Increasing dinoflagellate proportions steepened the slope during summer (r^2 = 0.443, p = 0.018). When functional groups were expressed as biomass rather than proportions of biomass, similar results were obtained.

Fig 1. Monthly mean values of (**a**) sea surface temperature and total biomass concentration within the major plankton functional groups, based on the 275-weekly time points spanning 2009–2014. Biomasses in all panels are plotted on the same logarithmic scale to illustrate the higher variability for some groups. For reference, the main stratification period is shaded gray. (**b**) Bacteria and picoplankton derived from flow cytometry. (**c**) Total nanoplankton derived by flow cytometry; that is, nanoflagellates, cryptophytes plus coccolithophores. (**d**) Total dinoflagellates from lugols counts. (**e**) Total diatoms, derived from Lugol's cell counts. (**f**) Total copepods. (**g**) Gelatinous zooplankton, that is, cnidarians and ctenophores.
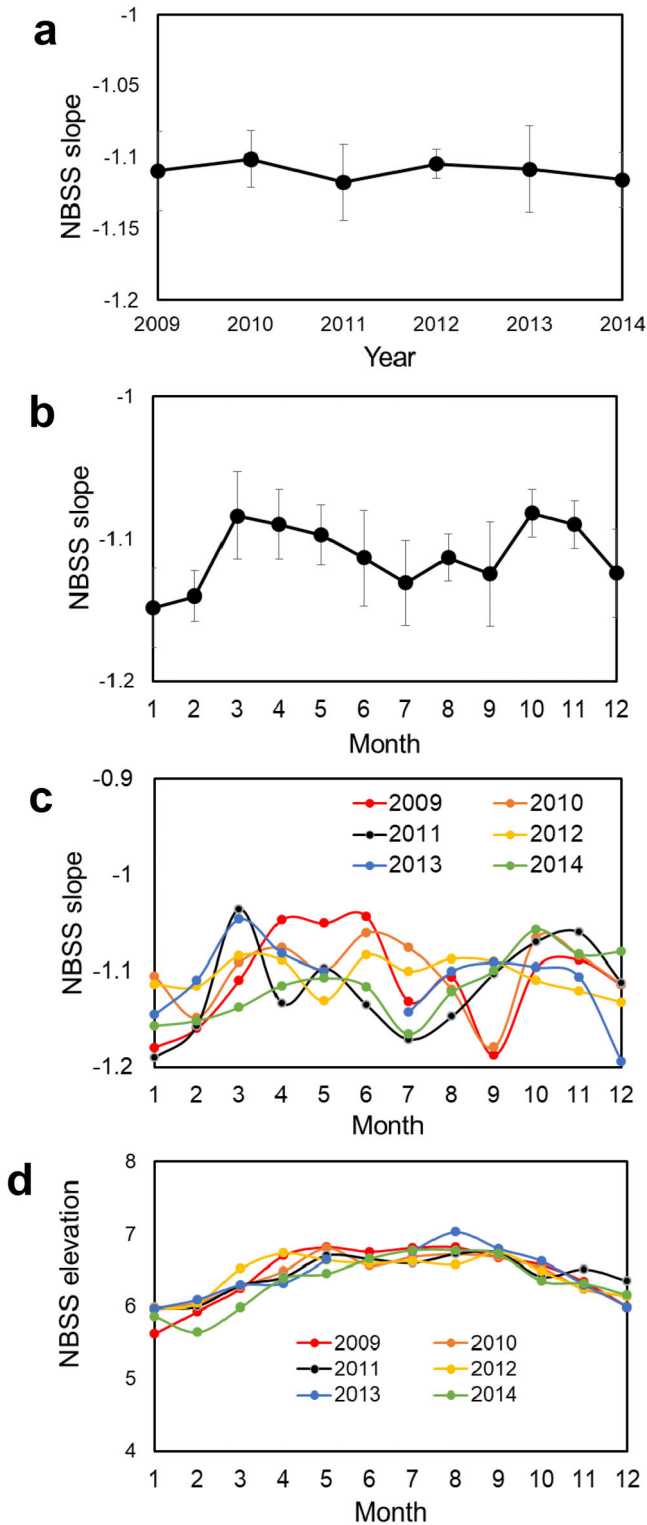
Fig 2. Seasonal-annual and interannual behavior of the L4 NBSS slope and elevation of the slope (presented as an index of biomass: see Methods). (**a**) Interannual variation in NBSS slope with bars as 95% confidence intervals based on the 6 study years. (**b**) Seasonal variation in NBSS slope (with 95% confidence intervals across the 6 years. (**c**) Monthly trajectories of NBSS slope in each year. (**d**) Corresponding NBSS elevations in each study year.

L4: Dome-shaped relationships between NBSS slope and plankton biomass

Steepening (more negative) NBSS slopes have been hypothesized to reflect warmer temperatures or reduced productivity (García-Comas et al. 2014) or alternatively increased productivity (San Martin et al. 2006*b*). The best fit to Chl *a* concentration was a dome shape, although this relationship was not significant. We find a much clearer dome-shaped relationship in Fig. 3a, between NBSS slope and the elevation of the NBSS (an internal proxy for biomass). Values toward the edge of this relationship (red symbols in Fig. 3a) reflect the storms spanning December 2013 to March 2014, whereby both the NBSS slope and elevation were initially depressed before quickly readjusting toward the apex of the dome after March 2014. The overall dome shape reflects repeating but partially mismatched seasonal cycles of slope and elevation of the NBSS.

The declining phase of the dome-shaped relationship between NBSS slope and elevation occurs during the main growth season (March to September) when water temperatures are rising and nutrients become depleted due to summer stratification. At this time, NBSS slope relates positively to the recent history of nutrient availability (Fig. 3b,c), showing the increasing importance of small taxa under warm, nutrient-stressed conditions. Despite the $10°C$ temperature range across the L4 time series, there was no direct relationship between NBSS slope and temperature (Fig. 3d). This suggests that changes in NBSS slope were driven instead by indirect temperature effects, for example, via stratification and nutrient supply (Fig. 3b,c).

Meta-analysis of the literature data: What methodological factors govern NBSS slopes?

In addition to our high frequency time series at a single station, we used a global-scale meta-analysis of the marine and freshwater plankton data to provide a larger scale perspective of the factors that modulate slopes of NBSS. Figure 4a places the range of monthly mean slopes of the NBSS at L4 into this wider context (Supporting Information Table S2). Overall, there is a funnel-shaped relationship, with high variability when studies measure across only a small ranges of body size. Fewer studies assess large ranges of mass or biovolume, but despite this disparity in sample size, it is clear that variability in NBSS slope decreases sharply when 7 orders of magnitude or more in organism mass are considered in the slope determination (vertical dashed line in Fig. 4a).

A second key result emerges from our literature compilation in Fig. 4a: the method used to derive the NBSS slope has a major bearing on its value. NBSS slopes based on biovolume (median −0.910) are significantly > −1, in contrast to those derived from mass units (median −1.131) which are significantly < −1 (Table 1).

Meta-analysis of literature data: What environmental factors govern NBSS slopes?

Most of the studies we compiled in Fig. 4a did not have concurrent data recorded on temperature, nutrients, primary
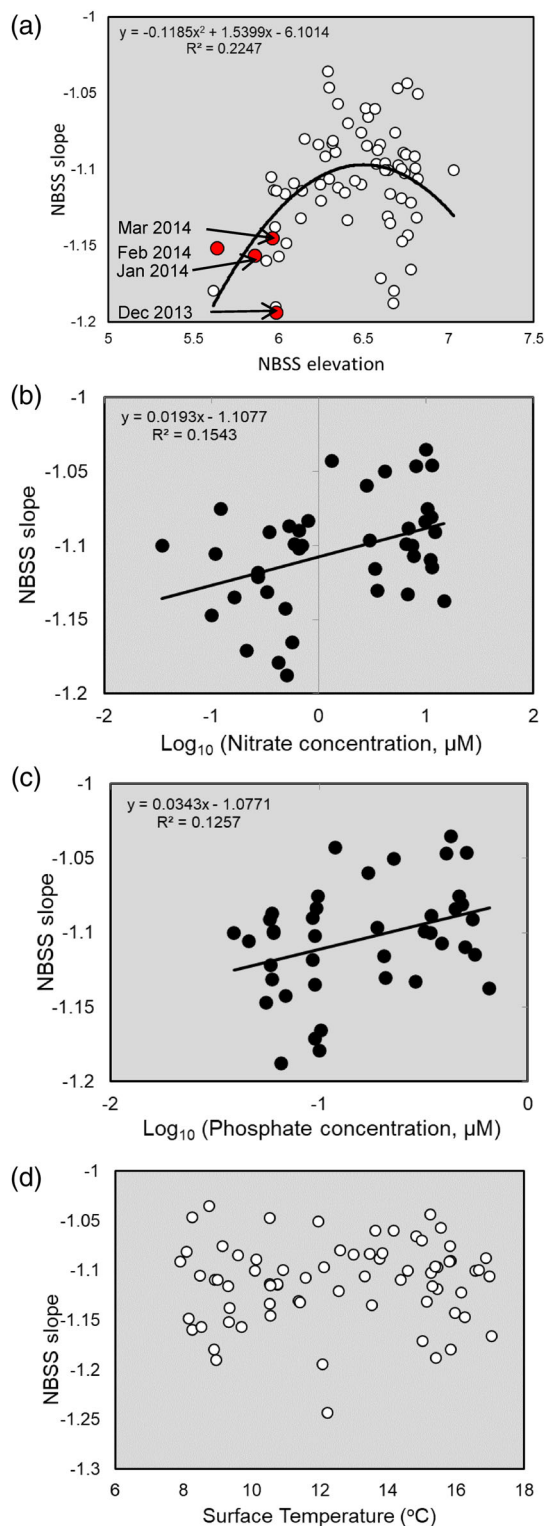
production, or phytoplankton concentrations. However, surface Chl *a* data were recorded for most of the marine studies where a large mass range was recorded, so we base the following analyses on these. Given the absence of consistently recorded temperature data, and the fact that the marine studies span the tropics to the poles in Atlantic and Pacific Oceans only, we have used latitude north or south as a crude proxy for thermal regime. Based on these marine data, NBSS shows no clear relationship with latitude, whether the slopes are based on mass or biovolume (Fig. 4b). Instead, Fig. 4b emphasizes the much steeper slope values of the mass-derived spectra as compared to those derived from biovolume (Table 1).

By contrast, these marine data spanning a large mass range showed a dome-shaped relationship with Chl *a* concentration (Fig. 4c). In common with the latitude data as a crude proxy for temperature, surface Chl *a* values provide only a very rough index of nutrient status and overall pelagic productivity. However, the Chl *a* values in Fig. 4c span 2 orders of magnitude, from highly oligotrophic ocean gyres to dense blooms, so they probably differentiate across the broad spectrum of nutrient supply. The lines of best fit for the individual studies in Fig. 4c show contrasting positive and negative relationships between NBSS slope and Chl *a* concentration depending on their position relative to the overall dome, highlighting the need to assess NBSS slopes across very wide ranges of productivity to assess the nature of this relationship.

Discussion

How do seasonality and climatic extremes impact on planktonic size structure?

The out-of-phase phenologies of NBSS slope and total plankton biomass emphasize the need to assess seasonality when interpreting size spectra. Single survey "snapshots" of NBSS during the ascending or descending portions of a seasonal dome-shaped relationship (Fig. 3a) could yield either positive or negative relationships between NBSS slope and elevation (i.e., biomass). This highlights the advantage of time-resolving sampling for a full assessment of size spectra (García-Comas et al. 2014; Sprules and Barth 2016).

Based on seasonal coverage, our expectation was that the spring bloom would introduce a pulse of mass to the base of the food web, leading to the steepest (most negative) NBSS

Fig 3. Interrelationships among monthly mean NBSS slopes, elevations and environmental variables at L4. Each point represents a monthly average value. (**a**) A significant dome-shaped relationship ($p = 0.002$, $n = 71$ months) between NBSS slope and elevation. Red points mark the months of the exceptionally stormy winter 2013/2014. (**b**) Significant relationship ($p = 0.011$, $n = 41$ months during the March–September growth season) between monthly NBSS slope and recent nutrient history, that is, surface nitrate concentrations averaged for the month of the NBSS slope determinations and the two preceding months. (**c**) The same plot as panel (**b**), but for phosphate ($p = 0.023$). (**d**) No relationship between NBSS slope and sea surface temperature.

slopes, as found by Gaedke (1992) in Lake Constance. We expected that biomass would then pass up into the higher trophic levels in the summer, helping to flatten the slope (Zhou

(a)

(b)

(c)

$$y = -0.1051x^2 - 0.0358x - 1.0964$$
$$R^2 = 0.4861$$

et al. 2009; Tarling et al. 2012). However, data collected at L4 are somewhat counter-intuitive, with shallow NBSS slopes just before the spring bloom, steepening toward late summer, and with steep slopes also during winter.

The counterintuitive NBSS behavior at L4 reflects several intriguing characteristics of this stratifying shelf site. The first feature is a surprising spring phenology, whereby mesozooplankton grazers increase in biomass earlier in spring than the diatom bloom (Atkinson et al. 2015; Fig. 1). This is a recurring feature at this site, likely reflecting adequate winter food, coupled to strong predation pressure later in the season (Atkinson et al. 2018; Cornwell et al. 2018; Maud et al. 2018). An influx of allochthonous carbon from meroplankton also helps to make March the month with a relatively flat NBSS slope.

Later in the summer, a second counterintuitive feature helps to drive a progressive steepening of the NBSS slope from March until early autumn. Although biomass of metazoan grazers increases throughout this period, the build-up is modest. By contrast there are substantial increases in pico- and nano-sized cells as well as dinoflagellates (Figs. 1, 2), despite the sustained low nutrient concentrations throughout summer (Smyth et al. 2010). This points to the importance of nutrient renewal; low-level pulses of nutrients throughout summer from riverine input, rainfall and wind mixing events, with rapid uptake by small cells keeping pace with supply to maintain low nutrient levels. These two processes, highlighted
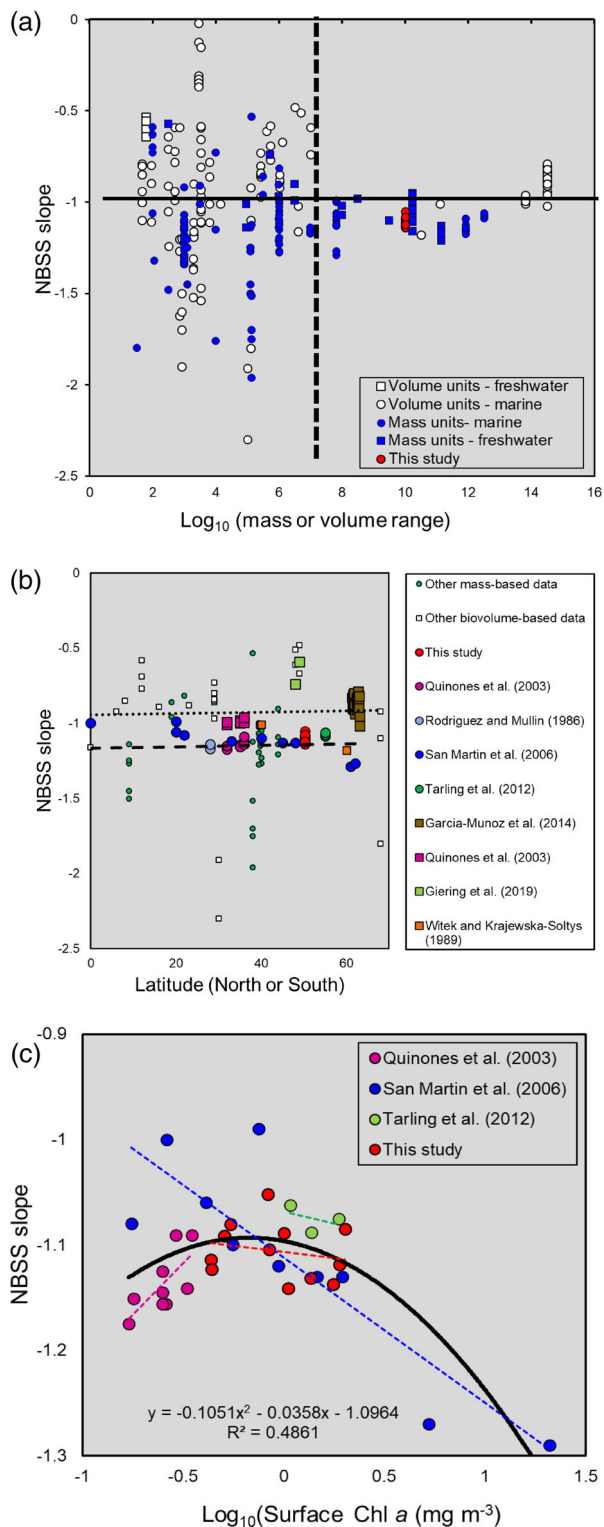
Fig 4. Meta-analysis of available aquatic literature on planktonic NBSS slopes. (**a**) Our monthly mean NBSS slope values, in the context of 282 values from 40 other marine and freshwater plankton studies compiled from the literature. Each data point is the average slope for a specific environment, for example a monthly average NBSS slope for a time series, or for a specific subregion of a spatial study (see Table 1 for summary statistics and Supporting Information Table S2 for more detailed description and values for each study). The *x*-axis represents the number of orders of magnitude of variability in range of mass or biovolume that is included in each study. The reference NBSS slope line is marked at −1 (see Table 1 for statistical comparisons of these data against this value). The vertical dashed line marks an approximate cut-off size range of 7 orders of magnitude, after which slope values become substantially less variable. (**b**) lack of any clear relationship between NBSS slopes for marine studies and latitude north or south, selected here as a crude proxy of water temperature at the global scale. Studies in legend are those where at least 7 orders of magnitude of mass or biovolume range were included (see panel a above). Smaller symbols are studies where 5–7 orders of magnitude were included. Circles are based on mass units and squares are based on biovolume. Nonsignificant lines of best fit (dashed for mass units and dotted for biovolume) are nearly horizontal, suggesting little underlying effects of latitude or temperature at global scales. (**c**) A significant (*p* < 0.001) dome-shaped relationship between NBSS slope and ambient Chl *a* concentration, based on comparable plankton studies measuring body mass and spanning at least 7 orders of magnitude of body mass. Dashed lines represent linear lines of best fit for each study. These 34 data points comprise 407 individual sampling stations or sampling time points. Removing the two outlying values with high Chl *a* values preserves the dome shape relation (*R*² = 14%, *n* = 32, *p* = 0.05).

Table 1. Summary statistics of our literature data compilation (Fig. 4, Supporting Information Table S2; see footnote for references used) comparing median values for NBSS for freshwater, marine, and all studies combined. Analyses are based on all available data and for those studies where at least 7 orders of magnitude of variation in carbon mass were measured, since this is considered as the most suitable indicator of NBSS slopes. Statistics are based on a Wilcoxon nonparametric one-sample test against a fixed NBSS slope value of −1.0. The data presented in volume units had a NBSS slope significantly > −1, while the remaining significant median values presented were < −1. NS: Not significant ($p > 0.05$). Number of obs. Is the number of distinct reported observations of size spectra (e.g., subregions or seasonal time points), although each of these frequently is an average of many more sampling time points or individual stations.

Group	Mass or volume range of data included	Median slope of NBSS	Number of obs.	Wilcoxon statistic	*p* value
In mass units	All data included	−1.131	149	1392	< 0.001
In volume units	All data included	−0.910	133	5953	< 0.001
Marine	All data included	−1.040	244	11,889	0.017
Freshwater	All data included	−1.050	38	267	NS
In mass units	Data with mass ≥ 10^7	−1.113	64	31	< 0.001

Literature sources: Baird et al. (2008), Dai et al. (2016, 2017), Décima et al. (2016), Frangoulis et al. (2017), Gaedke (1992), García et al. (1994), García-Comas et al. (2014), Garcia-Muñoz et al. (2014), Giering et al. (2019), Hikichi et al. (2018), Huntley et al. (1995), Kamenir (2017), Ke et al. (2018), Kimmel et al. (2006), Lebourges-Dhaussy et al. (2014), Marcolin et al. (2013), Matsumo et al. (2012), Mehner et al. (2018), Naito et al. (2019), Napp et al. (1993), Noguiera et al. (2004), Quinones et al. (2003), Rodriguez and Mullin (1986), San Martin et al. (2006a, 2006b), Sato et al. (2015), Schultes et al. (2012), Sheldon et al. (1972), Sourisseau and Carlotti (2006), Sprules and Barth (2016), Sprules and Goyke (1994), Sprules and Munawar (1986), Sprules et al. (1983), Tarling et al. (2012), Wallis et al. (2016), Witek and Krajewska-Soltys (1989), Zhou (2006), and Zhou et al. (2009, 2015).

by size-based analysis, are not captured in conceptual or simulation models of L4 seasonality (Atkinson et al. 2018). The models tend to overemphasize the spring diatom bloom, a relatively indistinct feature in the size spectra. Thus, the unexpected, out-of-phase seasonal cycles of the NBSS slope and elevation provide valuable and alternative insights into plankton dynamics.

The above discussion points to the key role of pico- and nano-sized cells and their mixo-heterotrophic grazers at L4, relative to the spring diatom bloom. The smaller cells dominate total biomass, yet are relatively stable in their biomass from year to year, helping to "anchor" the size structure of the assemblage. Their small size and efficient uptake of nutrients (Kiørboe 2008) trickles energy continually into a strongly size-structured planktonic food web. While this anchoring effect ensures that the NBSS slopes and elevations are remarkably similar between the 6 years (from −1.101 to −1.117; Fig. 2a), the biomasses of individual functional groups are highly variable, frequently varying by orders of magnitude between years in any given month (Fig. 1). For one of the most variable taxa, namely dinoflagellates, there is some imprint of this variation, as it has a significant levering effect on the slopes of the NBSS. However, this is not sufficient to cause significant interannual variation, from which we speculate that there is a degree of functional replacement in this food web based on body size. As suggested by García-Comas et al. (2014) and Mehner et al. (2018), low values of any single functional group can be compensated by increased biomass of others of similar size, preserving stability of the overall size structure.

These findings point to an underlying resilience in the size structure of the L4 assemblage, albeit with important seasonality. This resilience is exemplified by the response to the series of storms that severely impacted the southwest United Kingdom from December 2013 to March 2014. These storms initially perturbed the size spectrum by severely reducing metazoan densities to the lowest values seen over the whole six-year period (Fig. 1). Fortuitously, copepod mortality was also monitored over this period, and the storms coincided with a rapid increase in non-consumptive mortality of the key copepod *Calanus helgolandicus* (Maud et al. 2018). Mortality was linked statistically to high wind-speed, with the authors invoking extreme turbulence and physical damage as the likely cause. A key finding of our study, however, is the rapid rebound of planktonic biomass and size structure after the extreme weather. This provides additional evidence for an inbuilt stability, and tight coupling, in this size-structured system.

What do size spectra tell us about the efficiency of energy flow through the food web?

Equation 1 links the slope of the NBSS to the TTE, PPMR, and the coefficient that describes the body mass scaling of production (growth rate), *b*. Together they all contribute to an overall inefficiency in energy transfer across the planktonic size spectrum, compared to the benchmark values of TTE = 0.1, PPMR = 10^4, and $b = 0.75$ which would combine in Eq. 1 to yield a NBSS slope of − 1. The value of the body mass scaling coefficient of growth ($b = 0.75$; Brown et al. 2004) appears a reasonable approximation in marine pelagic organisms (Kiørboe and Hirst 2014). However, we do not know which combination of TTE and PPMR deviates from the above values to yield NBSS slopes < −1. Based on the above values, our

NBSS slopes steepening from −1.084 (March) to −1.131 (July) would translate to PPMR reducing from 986 (March) to 421 (July). Alternatively, it would translate to a seasonal decrease in TTE from 4.6% to 3.0%. Our meta-analysis based on mass-units shows slopes closer to the above-mentioned July values for L4, suggesting that PPMR and TTE values may indeed be much lower than their commonly quoted benchmark values. However, our seasonal L4 study shows that systematic shifts in slope may also occur as a result of perturbations in a system (e.g., blooms and mortality events). Such events break the assumptions of the biomass spectra being in a steady state, as underlying the mathematical models that describe the slope as a result of energy transfer processes. While our study emphasizes the need for seasonal- and large-scale integration, they also illustrate the benefit of using NBSS slopes to quantify the overall inefficiency of energy transfer across a wide size spectrum. It is a single, quantifiable index for a combination of three separate loss processes, each of which is extremely difficult to measure in whole assemblages (Jennings et al. 2002).

However, measuring a NBSS slope presents its own challenges, one of which is the choice of units. Quinones et al. (2003) found that their NBSS slope steepened by 0.15 if expressed in carbon units rather than as biovolume, so they warned against over-interpreting small variations in slopes of biomass spectra between different studies. We found an even larger difference (0.221) in our literature comparison (Fig. 4, Table 1). Median NBSS slopes based on biomass (− 1.131, n = 149) were significantly steeper than those based on biovolume (−0.910, n = 133, Mann–Whitney test, $p < 0.001$). This is a substantial difference; once again keeping the PPMR = 10^4 and b = 0.75, it would translate to a median TTE = 23% if based on biovolume or 3.0% if based on carbon mass. The latter is closer to directly determined values (Mehner et al. 2018) and we suggest that carbon mass units are more representative of metabolically active biomass than body volume. The discrepancy in the slopes may have several causes, one of which is the greater tissue dilution by water (i.e., gelatinousness) of zooplankton taxa with increasingly high carbon masses (McConville et al. 2017).

In addition to the choice of measurement units, there are serious challenges in measuring the full size-spectrum at sufficient spatial and temporal scales. Our meta-analysis shows wide scatter when only a small portion of the size spectrum is measured. As the authors of these studies acknowledge, the slopes may not always be fully representative of the studied systems. Instead, they may reflect "snapshots" of portions of the NBSS, and more heavily influenced by seasonality and internal dome-shaped structures (Rossberg 2012; Rossberg et al. 2019). Based on Fig. 4, a range of at least 7 orders of magnitude of body mass might be needed before this detail is averaged out. Nevertheless, Table 1 shows that steep NBSS slopes (i.e., significantly < −1), typify marine and freshwater habitats. Given the finding that some of these studies are based on biovolume and not carbon, and that the latter yield steeper slopes, our finding of steep (< −1) NBSS slopes at L4 is upheld more generally.

The L4 study site, in providing a seasonal dimension to the NBSS values, provides some clues into the cause of the pelagic food web inefficiency. Bentho-pelagic coupling at L4 is strong, with a rich benthic fauna supported by settled, often-fresh phytoplankton (Tait et al. 2015; Zhang et al. 2015). Despite inputs of meroplankton mainly in spring and seaweed detritus in autumn (Quierós et al. 2019), there is probably a net organic carbon loss from the water column, from vertical flux and the uptake of water column material by benthic organisms, contributing to low overall values of pelagic TTE.

A key feature at L4 is the summer time steepening of the NBSS slope related to progressive nutrient stress, and we speculate that low predator–prey size ratios play a part in this. A series of data compilations from the aquatic literature all point to a general increase of PPMR with predator size (Hansen et al. 1994; Kiørboe 2008; Barnes et al. 2010; Atkinson et al. 2014; Brose et al. 2019). Converted here by cubing from their original linear dimensions to approximate mass ratios, Hansen et al. (1994) showed that PPMRs increased from 1:1 for a dinoflagellate species, to 27:1 for other flagellates, to 512:1 for ciliates to 5832:1 for rotifers and copepods, up to 125,000:1 for cladocerans and meroplankton larvae. The picoplankton also fit into the bottom of this PPMR range. For instance, *Micromonas pusilla*, a dominant eukaryotic picoplankter in the western English Channel (Not et al. 2004), has PPMRs of ~ 15:1 (McKie-Krisberg and Sanders 2014). Increasing PPMRs with body size have also been found across copepods, krill and small fish (Atkinson et al. 2014) and among larger fish (Barnes et al. 2010). Because linear regressions provided good fits for our NBSS data, which were always measured across the same size range, any systematic increase in PPMR with body size would presumably need to be compensated by a decrease in TTE to ensure that linearity is maintained (Barnes et al. 2010). Notwithstanding this complication, the wide range in PPMRs that have been reported across the planktonic size spectrum suggests that seasonal variation in these values influences the NBSS slopes.

What can size spectra tell us about climate change responses?

Clearly, size spectrum approaches have limitations. They cannot resolve important species-specific detail, for example on changing distribution patterns or replacement of nutritious taxa with those of similar size, but which are non-nutritious or harmful (Schmidt et al. 2020). Their key advantage is that, when based on time averaging measurements, and across a sufficiently large range of body mass, they provide insights into some key properties of the system. The efficiency of transfer from primary producers to valuable planktivores such as fish may change in future climates, and size spectrum approaches can diagnose these changes.
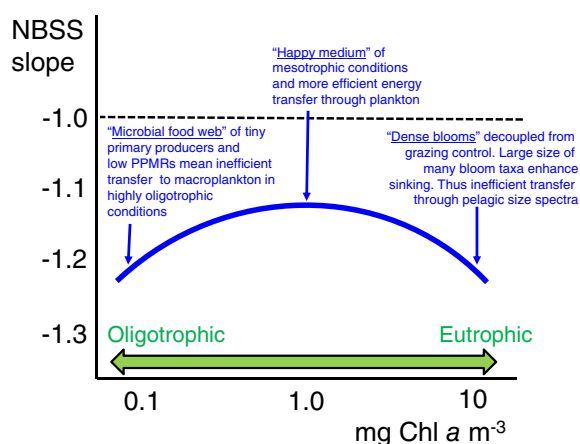
Fig 5. Our hypothesized relationship between NBSS slope and trophic status (indexed by approximate Chl *a* concentration on the *x*-axis). This concept pertains to marine planktonic systems and is based on a series of dome-shaped relationships emerging in Figs. 3 and 4. Importantly, the overall NBSS slopes based on mass units are significantly < −1 (Table 1), with steepest slopes (i.e., most inefficient energy transfer across the planktonic size spectrum) suggested at extremes of oligotrophy or eutrophy.

Warming oceans may have both direct and indirect effects on the size structure of plankton. Because temperature has direct effects on metabolism, and these effects scale with body size (Brown et al. 2004), NBSS slopes have been hypothesized to steepen in warmer environments (García-Comas et al. 2014). Neither our time series (Fig. 3a) nor our meta-analysis (Fig. 4b) provided support for this, and as found by García-Comas et al. (2014), any direct temperature effect seems to be outweighed by indirect effects, via changes in nutrient supply influencing food web structure.

These indirect effects were manifested by a series of dome-shaped relationships between NBSS and plankton biomass based on time series (Fig. 3a) and the meta-analysis (Fig. 4c). In Fig. 5, we speculate that separate but counteracting mechanisms govern the left and right portions of this dome. For its left-hand, oligotrophic, portion the L4 time series study provides a natural experiment in how progressive nutrient starvation throughout summer depresses the efficiency of the food web (Fig. 3b,c). This echoes findings in the Great Lakes by Sprules and Munawar (1986), who suggested that NBSS slopes can be used as an index of nutrient status. Building on these observations and theory (e.g., Jennings and Mackinson 2003), we suggest that in increasingly stable and oligotrophic systems, picoplankton dominate the primary production (Morán et al. 2010) driving the microbial loop, low PPMRs and substantial energy loss through long, inefficient food chains.

Eutrophic systems, by contrast, may form the right-hand side of the putative dome. These feature dense blooms of large, often unpalatable, or harmful algae (e.g., large diatoms, dinoflagellates or *Phaeocystis* spp.) which are decoupled from grazing control (Irigoien et al. 2005). Their typically large cell

or colony size also enhances the chances of mass-sinking of ungrazed blooms (Turner 2002). In combination, these factors would lead to relatively inefficient transfer to grazers (San Martin et al. 2006*b*). Indeed, our suggestion of a dome-shaped relationship helps to rationalize seemingly conflicting reports of positive- (Sprules and Munawar 1986), negative (San Martin et al. 2006*a*, *b*) and no relationships (Kenitz et al. 2018) between size structure and productivity indices. As shown in Fig. 4c, the sign of the relationship for any regional- or time-restricted study would depend on where the measurements lay, relative to the dome.

Future perspectives

In summary, our time series and meta-analysis show that three conditions must ideally be met for empirical studies to quantify the efficiency of energy flow through the planktonic size spectrum. First, size spectra are preferably based on mass rather than on biovolume, since the former relates more closely to energy and because zooplankton mass and volume do not scale linearly (McConville et al. 2017). Second, they should include a mass range ideally of at least ~ 7 orders of magnitude, to include small phytoplankton as well as zooplankton. Third, they need to include a degree of spatial and/or temporal integration, as short-term snapshots can be misleading. None of these suggestions are new (e.g., Quinones et al. 2003; San Martin et al. 2006*b*; Andersen and Pedersen 2010; Sprules and Barth 2016), but we believe that Fig. 4c may be the first attempt to combine the 407 individual measurements that fulfill these criteria to address macroscale patterns.

At these large scales of space and time, a key result of our study was a relatively steep overall slope of the NBSS. This value, −1.113, translates via Eq. 1 to a TTE of only 3.5% or a PPMR of only 569 (or more likely some less severely depressed combination of each of the two parameters). These are far lower than commonly used "benchmark" values of respectively 10% (Lindeman 1942) and 10,000 (Mehner et al. 2018). Andersen (2019) summarized respective values of 14% and ~ 700, so these large discrepancies underline the need for a better appreciation of food web transfer efficiency, key to a variety of size-based models (e.g., Banas 2011; Ward et al. 2012; Blanchard et al. 2017). The insights on overall food web efficiency derived from syntheses of suitable size spectra are particularly valuable, given the great difficulty of directly determining overall values for PPMR and TTE in real food webs (Brose et al. 2019). As well as setting likely boundaries for realistic combinations of TTE and PPMR for plankton, our speculated dome-shaped relationship between NBSS and plankton biomass may help to rationalize ongoing debates over whether this relationship is positive, negative or absent.

With rising temperatures, an increase in stratification and nutrient stress for mid-latitudes is widely projected (Holt et al. 2016; IPCC 2019). In tandem, these conditions are commonly considered to favor small primary producers

(Li et al. 2009; Morán et al. 2010). Such changes are already being observed (Schmidt et al. 2020) and are concomitant with changing human nutrient inputs to inshore eutrophic waters (Capuzzo et al. 2018). Such shifts underline the need to better understand how pelagic food web efficiency relates to nutrient status. We hope that our initial synthesis of published size spectra (Supporting Information Table S2) forms a building block for those aiming toward a more advanced analysis of these key macroecological patterns, including an improved comparison of marine and freshwater realms.

Because size spectra are measurable in ways that can be made intercomparable between systems or across time, they may provide a quantitative index of ecosystem health and resilience; hallmarks of the "Good Environmental Status" targets for policy reporting (McQuatters-Gollop et al. 2019). This resilience was illustrated by the recovery of NBSS slopes from abnormally low values to normal values within a month of the series of exceptional storms. Size-based approaches therefore provide an index of resilience of systems to the sorts of climatic extremes that are widely projected for a warmer world (IPCC 2019).

References

Andersen, K. H. 2019. Fish ecology. Evolution and exploitation: Princeton, NJ, ISBN: 9780691176550.

Andersen, K. H., and M. Pedersen. 2010. Damped trophic cascades driven by fishing in model marine ecosystems. Proc. R. Soc. B **277**: 795–802. doi:10.1098/rspb.2009.1512

Atkinson, A., S. H. Hill, M. Barange, E. A. Pakhomov, D. Raubenheimer, K. Schmidt, S. J. Simpson, and C. Reiss. 2014. Sardine cycles, krill declines and locust plagues: Revisiting "wasp-waist" food webs. Trends in Ecology and Evolution **29**: 309–316. doi:10.1016/j.tree.2014.03.011

Atkinson, A., R. A. Harmer, C. E. Widdicombe, A. J. McEvoy, T. J. Smyth, D. G. Cummings, P. J. Somerfield, J. L. Maud, and K. McConville. 2015. Questioning the role of phenology shifts and trophic mismatching in a planktonic food web. Prog. Oceanogr. **137**: 498–512. https://doi.org/10.1016/j.pocean.2015.04.023

Atkinson, A., L. Polimene, E. S. Fileman, C. E. Widdicombe, A. J. McEvoy, T. J. Smyth, N. Djeghri, S. F. Sailley, and L. E. Cornwell. 2018. What drives plankton seasonality in a stratifying shelf sea? Some competing and complementary theories. Limnol. Oceanogr. **63**: 2877–2884. doi:10.1002/lno.11036

Baird, M. E., P. G. Timko, J. H. Middleton, T. J. Mullaney, D. R. Cox, and I. M. Suthers. 2008. Biological properties across the Tasman front off Southeast Australia. Deep-Sea Res. I **55**: 1438–1465. doi:10.1016/j.dsr.2008.06.011

Banas, N. S. 2011. Adding complex trophic interactions to a size-spectral plankton model: Emergent diversity patterns and limits on predictability. Ecol. Model. **222**: 2663–2675. doi:10.1016/j.ecolmodel.2011.05.018

Barnes, C., D. Maxwell, D. C. Reuman, and S. Jennings. 2010. Global patterns in predator–prey size relationships reveal size dependency of trophic transfer efficiency. Ecology **91**: 222–232. doi:10.1890/08-2061.1

Blanchard, J. L., R. F. Heneghan, J. D. Everett, R. Trebilco, and A. J. Richardson. 2017. From bacteria to whales: Using functional size spectra to model marine ecosystems. Trends in Ecology and Evolution **32**: 174–186. https://doi.org/10.1016/j.tree.2016.12.003

Brose, U., and others. 2019. Predator traits determine food web architecture across ecosystems. Nat. Ecol. Evol. **3**: 919–927. doi:10.1038/s41559-019-0899-x

Brown, J. H., J. F. Gillooly, A. P. Allen, V. M. Savage, and G. B. West. 2004. Toward a metabolic theory of ecology. Ecology **85**: 1771–1789. doi:10.1890/03-9000

Capuzzo, E., et al. 2018. A decline in primary production in the North Sea over 25 years, associated with reductions in zooplankton abundance and fish stock recruitment. Global Change Biol. **24**: e352–e364. doi:10.1111/gcb.13916

Cornwell, L. E., and others. 2018. Seasonality of *Oithona similis* and *Calanus helgolandicus* reproduction and abundance: Contrasting responses to environmental variation at a shelf site. J. Plankton Res. **40**: 295–310. doi:10.1093/plankt/fby007

Coumou, D., and S. Rahmstorf. 2012. A decade of weather extremes. Nat. Climate Change **2**: 491–496. doi:10.1038/nclimate1452

Dai, L., C. Li, G. Yang, and X. Sun. 2016. Zooplankton abundance, biovolume and size spectra at western boundary currents in the subtropical North Pacific during winter 2012. J. Mar. Syst. **155**: 73–83. doi:10.1016/j.jmarsys.2015.11.004

Dai, L., C. Li, Z. Tao, G. Yang, X. Wang, and M. Zhu. 2017. Zooplankton abundance, biovolume and size spectra down to 3000m depth in the western tropical Pacific during autumn 2014. Deep-Sea Res. I. **121**: 1–13. doi:10.1016/j.dsr.2016.12.015

Daufresne, M., K. Lengfellner, and U. Sommer. 2009. Global warming benefits the small in aquatic ecosystems. Proc. Natl. Acad. Sci. **106**: 12788–12793. doi:10.1073/pnas.0902080106

Décima, M., M. R. Landry, M. R. Stukel, L. Lopex-Lopez, and J. W. Krause. 2016. Mesozooplankton biomass and grazing in the Costa Rica dome: Amplifying variability through the food web. J. Plankton Res. **38**: 317–330. doi:10.1093/plankt/fbv091

Edwards, A. M., J. P. W. Robinson, M. J. Plank, J. K. Baum, and J. L. Blanchard. 2017. Testing and recommending methods for fitting size spectra to data. Methods Ecol. Evol. **8**: 57–67. doi:10.1111/2041-210X.12641

Eloire, D., P. J. Somerfield, D. V. P. Conway, C. Halsband-Lenk, R. P. Harris, and D. Bonnet. 2010. Temporal variability and community composition of zooplankton at station L4 in the Western Channel: 20 years of sampling. J. Plankton Res. **32**: 657–679. doi:10.1093/plankt/fbq009

Elton, C. 1927. Animal ecology. Macmillan.

Frangoulis, C., M. Grigoratou, T. Zoulias, C. C. S. Hannides, M. Pantazi, S. Psarra, and I. Siokou. 2017. Expanding zooplankton standing stock estimation from micro- to meta-zooplankton: A case study in the N. Aegean Sea (Mediterranean Sea). Continent. Shelf Res. **149**: 151–161. doi:10.1016/j.csr.2016.10.004

Gaedke, U. 1992. The size distribution of plankton biomass in a large lake and its seasonal variability. Limnol. Oceanogr. **37**: 1202–1220. doi:10.4319/lo.1992.37.6.1202

García, C. M., and others. 1994. The size structure and functional composition of ultraplankton and nanoplankton at a frontal station in the Alboran Sea. Working Groups 2 and 3 report. Scientia Marina **58**: 43–52.

García-Comas, C., C.-Y. Chang, L. Ye, A. R. Sastri, and Y.-C. Lee. 2014. Mesozooplankton size structure in response to environmental conditions in the East China Sea: How does size spectra theory fit empirical data of a dynamic coastal area? Progr. Oceanogr. **121**: 141–157. doi:10.1016/j.pocean.2013.10.010

Garcia-Muñoz, C., C. M. Garcia, L. M. Lubián, A. López-Urrutia, S. Hernández-León, and J. Ameneiro. 2014. Metabolic state along a summer north–south transect near the Antarctic Peninsula: A size spectra approach. J. Plankton Res. **36**: 1074–1091. doi:10.1093/plankt/fbu042

Giering, S.L., Wells, S.R., Mayers, K.M.J., Shuster,H., Cornwell, L., Fileman, E., Atkinson, A., Cook, K.B., Preece, C., and D. J. Mayor. 2019. Seasonal variation of zooplankton community structure and trophic position in the Celtic Sea: A stable isotope and biovolume spectrum approach. Progr. Oceanogr. **177**: 101943. https://doi.org/10.1016/j.pocean.2018.03.012

Hansen, B., P. K. Bjornsen, and P. J. Hansen. 1994. The size ratio between planktonic predators and their prey. Limnol. Oceanogr. **39**: 395–403. doi:10.4319/lo.1994.39.2.0395

Harris, R. P. 2010. The L4 time series: The first 20 years. J. Plankton Res. **32**: 577–583. doi:10.1093/plankt/fbq021

Hikichi, H., D. Arima, Y. Abe, K. Matsumo, K. Hamaoka, S. Katakura, H. Kasai, and A. Yamaguchi. 2018. Seasonal variability of zooplankton size spectra at Mombetsu Harbour in the sothern Okhotsk Sea during 2011: An analysis using an optical plankton counter. Regional Studies Mar. Sci. **20**: 34–44. doi:10.1016/j.rsma.2018.03.011

Holt, J., and others. 2016. Potential effects of climate change on the primary production of regional seas: A comparative analysis of five European seas. Progr. Oceanogr. **140**: 91–115. doi:10.1016/j.pocean.2015.11.004

Huntley, M. E., M. Zhou, and W. Nordhausen. 1995. Mesoscale distribution of zooplankton in the California current in late spring, observed by optical plankton counter. J. Mar. Res. **53**: 647–674. doi:10.1357/0022240953213061

IPCC. 2019. Summary for policymakers. (In press), 198pp. In H.-O. Pörtner et al. [eds.], *IPPC* Special Report on the Ocean and Cryosphere in a Changing Climate. Intergovernmental Panel on Climate Change.

Irigoien, X., K. J. Flynn, and R. P. Harris. 2005. Phytoplankton blooms: A "loophole" in microzooplankton grazing impact? J. Plankton Res. **27**: 313–321. doi:10.1093/plankt/fbi011

Jennings, S., and S. Mackinson. 2003. Abundance-body mass relationships in size-structured food webs. Ecol. Lett. **6**: 971–974. doi:10.1046/j.1461-0248.2003.00529.x

Jennings, S., K. J. Warr, and S. Mackinson. 2002. Use of size-based production and stable isotope analyses to predict trophic transfer efficiencies and predator–prey body mass ratios in food webs. Mar. Ecol. Progr. Ser. **240**: 11–20. doi:10.3354/meps240011

Kamenir, Y. 2017. The living whirl self-maintenance of stable size structure patterns of aquatic communities. Int. J. Environ. Prot. **7**: 46–52. doi:10.5963/IJEP0701005

Ke, Z. X., Y. H. Tan, L. M. Huang, J. X. Liu, and H. X. Liu. 2018. Community structure and biovolume size spectra of mesozooplankton in the pearl river estuary. Aquat. Ecosyst. Health Manage. **21**: 30–40. doi:10.1080/14634988.2018.1432948

Kendon, M., and M. McCarthy. 2015. The UK's wet and stormy winter of 2013/2014. Weather **2015**: 40–47. doi:10.1002/wea.2465

Kenitz, K. M., A. W. Visser, M. D. Ohman, M. R. Landry, and K. H. Andersen. 2018. Community trait distribution across environmental gradients. ECOSYSTEMS **22**(5): 968–980. doi:10.1002/wea.2465

Kimmel, D. G., M. R. Roman, and X. Zhang. 2006. Spatial and temporal variability in factors affecting mesozooplankton dynamics in Chesapeake Bay: Evidence from biomass spectra. Limnol. Oceanogr. **51**: 131–141. doi:10.4319/lo.2006.51.1.0131

Kiørboe, T. 2008. A mechanistic approach to plankton ecology. Princeton University Press, 209 pp. doi:10.1007/s00442-007-0893-x

Kiørboe, T., and A. G. Hirst. 2014. Shifts in mass scaling of respiration, feeding, and growth rates across life-form transitions in marine pelagic organisms. Am. Nat. **183**: E118–E130. doi:10.1086/675241

Lebourges-Dhaussy, A., J. Huggett, S. Ockuis, G. Roudaut, E. Josse, and H. Verheye. 2014. Zooplankton size and distribution within mesoscale structures in the Mozambique Channel: A comparative approach using the TAPS acoustic profiler, a multiple net sampler and ZooScan image analysis. Deep-Sea Res. II **100**: 136–152. doi:10.1016/j.dsr2.2013.10.022

Li, W.K.W., McLughlin, F.A., Lovejoy, C., Carmack, E.C. (2009). Smallest algae thrive as the Arctic Ocean freshens. Science, **326**: 539, 5952, doi:10.1126/science.1179798

Lindeman, R. L. 1942. The trophic-dynamic aspect of ecology. Ecology **23**: 802–811.

Marcolin, C.d. R., S. Schultes, G. A. Jackson, and R. Lopes. 2013. Plankton and seston size spectra estimated by the LOPC and ZooScan in the Alrolhos Bank ecosystem (SE Atlantic). Continent. Shelf Res. **70**: 74–87. doi:10.1016/j.csr.2013.09.022

Masselink, G., T. Scott, T. Poate, P. Russell, M. Davidson, and D. Conley. 2016. The extreme 2013/2014 winter storms: Hydrodynamic forcing and coastal response along the southwest coast of England. Earth Surf. Process. Landforms **41**: 378–391. doi:10.1002/esp.3836

Matsumo, K., A. Yamaguchi, and I. Imai. 2012. Biomass size spectra of mesoplankton in the Chukchi Sea during the summers of 1991/1992 and 2007/2008: An analysis using optical plankton counter data. ICES J. Mar. Sci. **69**: 1205–1217. doi:10.1093/icesjms/fss119

Maud, J. L., A. G. Hirst, A. Atkinson, P. Lindeque, and A. McEvoy. 2018. Mortality of *Calanus helgolandicus*: Sources, differences between the sexes and consumptive and non-consumptive processes. Limnol. Oceanogr **63**: 1741–1761. doi:10.1002/lno.10805

McConville, K., A. Atkinson, E. S. Fileman, J. I. Spicer, and A. G. Hirst. 2017. Disentangling the counteracting effects of water content and carbon mass on zooplankton growth. J. Plankton Res. **39**: 246–256. doi:10.1093/plankt/fbw094

McKie-Krisberg, Z., and R. W. Sanders. 2014. Phagotrophy by the picoeukaryotic green alga *Micromonas*: Implications for Arctic oceans. ISME J. **8**: 1953–1961. doi:10.1038/ismej.2014.16

McQuatters-Gollop, A., and others. 2019. Plankton lifeforms as a biodiversity indicator for regional-scale assessment of pelagic habitats for policy. Ecol. Indicat. **101**: 913–925. doi:10.1016/j.ecolind.2019.02.010

Mehner, T., B. Lischke, K. Scharnweber, K. Attermeyer, S. Brothers, U. Gaedke, S. Hilt, and S. Brucet. 2018. Empirical correspondence between trophic transfer efficiency in freshwater food webs and the slope of their size spectra. Ecology **99**: 1463–1472. doi:10.1002/ecy.2347

Morán, X. A. G., A. López-Urrutia, A. Calvo-Díaz, and W. K. W. Li. 2010. Increasing importance of small phytoplankton in a warmer ocean. Global Change Biol. **16**: 1137–1144. doi:10.1111/j.1365-2486.2009.01960.x

Naito, A., Y. Abe, K. Matsuno, B. Nishizawa, N. Kanna, S. Sugiyama, and A. Yamaguchi. 2019. Surface zooplankton size and taxonomic composition in Bowdoin Fjord, North-Western Greenland: A comparison of ZooScan, OPC and microscopic analysis. Polar Sci. **19**: 120–129. doi:10.1016/j.polar.2019.01.001

Napp, J. M., P. B. Ortner, R. E. Pieper, and D. V. Holliday. 1993. Biovolume-size spectra of epipelagic zooplankton using a multifrequency acoustic profiling system (MAPS). Deep-Sea Res. I **40**: 445–459. doi:10.1016/0967-0637(93)90141-0

Noguiera, E., González-Nuevo, Bode, A., Varela, M., Morán, X. A.G., and L. Valdes. 2004. Comparison of biomass and size spectra derived from optical plankton counter data and net samples: Application to the assessment of mesoplankton distribution along the northwest and northern Iberian shelf. ICES J. Mar. Sci. **1**: 508–517. doi:10.1093/plankt/fbw094

Not, F., M. Latasa, D. Marie, T. Cariou, D. Vaulot, and N. Simon. 2004. A single species, *Micromonas pusilla* (Prasinophyceae), dominates the eukaryotic picoplankton in the Western English Channel. Appl. Environ. Microbiol. **70**: 4064–4072. doi:10.1128/AEM.70.7.4064-4072.2004

Peters, R. H. 1983. The ecological implications of body size. Cambridge University Press.

Platt, T., and K. Denman. 1978. The structure of pelagic marine ecosystems. Rapp. P,-V. Reun. Cons. Int. Explor. Mer. **173**: 60–65.

Quierós, A. M., et al. 2019. Connected macroalgal-sediment systems: blue carbon and food webs in the deep coastal ocean. Ecol. Monogr. **89**(3): e01366. doi:10.1002/ecm.1366

Quinones, R. A., T. Platt, and J. Rodriguez. 2003. Patterns of biomass-size spectra from oligotrophic waters of the Northwest Atlantic. Progr. Oceanogr. **57**: 405–427. doi:10.1016/S0079-6611(03)00108-3

Reuman, D. C., C. Mulder, D. Raffaelli, and J. E. Cohen. 2008. Three allometric relations of population density to body mass: Theoretical integration and empirical tests in 149 food webs. Ecol. Lett. **11**: 1216–1228. doi:10.1111/j.1461-0248.2008.01236.x

Rodriguez, J., and M. M. Mullin. 1986. Relation between biomass and body weight of plankton in a steady state oceanic environment. Limnol. Oceanogr. **31**: 361–370. doi:10.4319/lo.1986.31.2.0361

Rossberg, A. G. 2012. A complete analytic theory for structure and dynamics of populations and communities spanning wide ranges in body size. Adv. Ecol. Res. **46**: 427–521. doi:10.1016/B978-0-12-396992-7.00008-3

Rossberg, A. G., U. Gaedke, and P. Kratina. 2019. Dome patterns in pelagic size spectra reveal strong trophic cascades. Nat. Commun. **10**: 4396. doi:10.1038/s41467-019-12289-0

San Martin, E., R. P. Harris, and X. Irigoien. 2006*a*. Latitudinal variation in plankton size spectra in the Atlantic Ocean. Deep-Sea Res. II: 1560–1572. doi:10.1016/j.dsr2.2006.05.006

San Martin, E., X. Irigoien, R. P. Harris, Á. López-Urrutia, M. V. Zubkov, and J. L. Heywood. 2006*b*. Variation in the transfer of energy in marine plankton along a productivity gradient in the Atlantic Ocean. Limnol. Oceanogr. **51**: 2084–2091 doi:10.4319/lo.2006.51.5.2084.

Sato, K., K. Matsuno, D. Arima, Y. Abe, and A. Yamaguchi. 2015. Spatial and temporal changes in zooplankton abundance, biovolume, and size spectra in the neighboring waters of Japan: Analyses using an optical plankton counter. Zool. Studies **54**: 18. doi:10.1186/s40555-014-0098-z

Schmidt, K., and others. 2020. Increasing picocyanobacteria success in shelf waters contributes to long-term food web degradation. Global Change Biol. doi:10.1111/gcb.15161

Schultes, S., Sourisseau, M., Le Masson, E., Lunven, M., and L. Marié. 2012. Influence of physical forcing on mesozooplankton at the Ushant tidal front. J. Mar. Syst. **109–110**, S191, S202. doi:10.1016/j.jmarsys.2011.11.025

Sheldon, R. W., W. H. Sutcliff, and A. Prakash. 1972. The size distribution of particles in the ocean. Limnol. Oceanogr. **17**: 327–340. doi:10.4319/lo.1972.17.3.0327

Smyth, T., A. Atkinson, S. Widdicombe, M. Frost, I. Allen, J. Fishwick, A. Queiros, D. Sims, and M. Barange. 2015. The western channel observatory. Progr. Oceanogr. **137**: 335–341. doi:10.1016/j.pocean.2015.05.020

Smyth, T. J., J. R. Fishwick, L. Al-Moosawi, D. G. Cummings, C. Harris, V. Kitidis, A. P. Rees, V. Martinez-Vicente, and E. M. S. Woodward. 2010. A broad spatio-temporal view of the Western English Channel observatory. J. Plankton Res. **32**: 585–601. doi:10.1093/plankt/fbp128

Sourisseau, M., and F. Carlotti. 2006. Spatial distribution of zooplankton size spectra on the French continental shelf of the Bay of Biscay during spring 2000 and 2001. J. Geophys. Res. **111**: C05509. doi:10.1029/2005JC003063

Sprules, W. G., J. M. Casselman, and B. J. Shuter. 1983. Size distribution of pelagic particles in lakes. Can. J. Fish. Aquat. Sci. **40**: 1761–1769. doi:10.1139/f83-205

Sprules, W. G., and M. Munawar. 1986. Plankton size spectra in relation to ecosystem productivity, size and perturbation. Can. J. Fish. Aquat. Sci. **43**: 1789–1794. doi:10.1139/f86-222

Sprules, W. G., and A. Goyke. 1994. Size-based structure and production in the pelagia of lakes Ontario and Michigan. Can, F. Fish. Aquat. Sci. **51**: 2603–2611. doi:10.1139/f94-260

Sprules, W. G., and L. E. Barth. 2016. Surfing the biomass size spectrum: Some remarks on history, theory, and application. Can. J. Fish. Aquat. Sci. **73**: 477–495. doi:10.1139/cjfas-2015-0115

Tait, K., R. L. Airs, C. E. Widdicombe, G. A. Tarran, M. R. Jones, and S. Widdicombe. 2015. Dynamic responses of the bacterial community at the Western English Channel Observatory site L4 are driven by deposition of fresh phyto-detritus. Progr. Oceanogr. **137**: 546–558. doi:10.1016/j.pocean.2015.04.020

Tarling, G. A., G. Stowasser, P. Ward, A. J. Poulton, M. Zhou, and H. J. Venables. 2012. Seasonal trophic structure of the Scotia Sea pelagic ecosystem considered through biomass spectra and stable isotope analysis. Deep-Sea Res. II **59–60**: 222–236. doi:10.1016/j.dsr2.2011.07.002

Tarran, G. A., and J. T. Brunn. 2015. Nanoplankton and picoplankton of the Western English Channel: Abundance and seasonality from 2007–2013. Progr. Oceanogr **137**: 446–455. doi:10.1016/j.pocean.2015.04.024

Trebilco, R., J. K. Baum, A. K. Salomon, and N. Dulvy. 2013. Ecosystem ecology: Size-based constraints on the pyramids of life. Trends Ecol. Evol. **28**: 423–431. doi:10.1016/j.tree.2013.03.008

Turner, J. T. 2002. Zooplankton fecal pellets, marine snow and sinking phytoplankton blooms. Aquat. Microb. Ecol. **27**: 57–102. doi:10.3354/ame027057

Wadey, M. P., I. D. Haigh, and J. M. Brown. 2014. A century of sea level data and the UK's 2013/14 storm surges: An assessment of extremes and clustering using the Newlyn tide gauge record. Ocean Sci. **10**: 1031–1045. doi:10.5194/os-10-1031-2014

Wallis, R. J., and others. 2016. Zooplankton abundance and biomass size spectra in the East Antarctic Sea-ice zone during the winter–spring transition. Deep-Sea Res. II **131**: 170–181. doi:10.1016/j.dsr2.2015.10.002

Ward, B. A., S. Duthiewicz, O. Jahn, and M. J. Follows. 2012. A size-structured food web model for the global ocean. Limnol. Oceanogr. **57**: 1877–1891. doi:10.4319/lo.2012.57.6.1877

Widdicombe, C. E., D. Eloire, D. Harbour, R. P. Harris, and P. J. Somerfield. 2010. Long-term phytoplankton community dynamics in the Western English Channel. J. Plankton Res. **32**: 643–655. doi:10.1093/plankt/fbp127

Witek, Z., and A. Krajewska-Soltys. 1989. Some examples of the epipelagic plankton size structure in high latitude oceans. J. Plankton Res. **11**: 1143–1155. doi:10.1093/plankt/11.6.1143

Zhang, Q., R. M. Warwick, C. L. McNeill, C. E. Widdicombe, A. Sheehan, and S. Widdicombe. 2015. An unusually large phytoplankton bloom drives rapid changes in benthic diversity and ecosystem function. Progr. Oceanogr. **137**: 533–545. doi:10.1016/j.pocean.2015.04.029

Zhou, L., L. Huang, Y. Tan, X. Lian, and K. Li. 2015. Size-based analysis of a zooplankton community under the influence of the pearl river plume and coastal upwelling in the north-eastern South China Sea. Marine Biol. Res. **11**: 168–179. doi:10.1080/17451000.2014.904882

Zhou, M. 2006. What determines the slope of a plankton bio-mass spectrum? J. Plankton Res. **28**: 437–448. doi:10.1093/plankt/fbi119

Zhou, M., and M. E. Huntley. 1997. Population dynamics theory of plankton based on biomass spectra. Mar. Ecol. Prog. Ser. **159**: 61–73. doi:10.3354/meps159061

Zhou, M., K. Tande, Y. Zhu, and S. Basedow. 2009. Productivity, trophic levels and size spectra of zooplankton in northern Norwegian shelf regions. Deep-Sea Res. II **56**: 1934–1944. doi:10.1016/j.dsr2.2008.11.018

Conflict of interest

None declared.

Data availability statement

Data from the L4 time series are available via the data tab on the Western Channel Observatory website https:// westernchannelobservatory.org.uk/ . Doi's for the specific data sets used in this study are provided in the Supporting Information Appendix S1. Supporting Information Table S2 contains the source data compiled from the literature.